

# Exploring the Potential of Graphene in Real-Life Industrial Anticorrosive Coatings

Xavier Raby<sup>a\*</sup> , Rafael Dias da Silva<sup>a</sup> 

<sup>a</sup>Gerdaug Graphene, 05424-050, São Paulo, SP, Brasil.

Received: November 30, 2023; Revised: February 27, 2024; Accepted: February 29, 2024

This study aims to provide clarity on the potential of graphene in real-life coatings applications and can be viewed as guidelines for graphene end users. To illustrate this, examples of different industrial applications are presented, where graphene-based additives demonstrate a significant impact on corrosion resistance. Furthermore, the underlying mechanisms behind these new products are elucidated.

**Keywords:** *Graphene, corrosion, coating, composite.*

## 1. Introduction

Graphene consists of a single atomic layer of sp<sup>2</sup> hybridized carbon atoms arranged in a honeycomb lattice<sup>1</sup>, rendering it the thinnest known 2D material with a thickness of 0.335 nm<sup>2</sup> with an impressive theoretical specific surface area of approximately 2630 m<sup>2</sup>.g<sup>-1</sup><sup>3</sup>. It can be viewed as the basic building block of the other sp<sup>2</sup> hybridized carbon nanostructures as they all emanate from the two-dimensional structure of graphene. For instance, introducing pentagons into the lattice creates positive curvature defects, resulting in structures such as fullerene<sup>4</sup>. Rolling a graphene sheet forms a carbon nanotube<sup>5</sup>, while stacking multiple layers of graphene leads to graphite<sup>6</sup>, as illustrated in Figure 1. Its extraordinary properties, reported in Table 1, are a direct result of its unique structure and electronic configuration. The strong in-plane covalent sp<sup>2</sup> bonds between adjacent carbon atoms, slightly stronger than sp<sup>3</sup> bonds in diamond, combined with the honeycomb atomic arrangement result in the remarkable stiffness of graphene<sup>9</sup> while keeping a low density ( $\leq 2,26 \text{ g.cm}^{-3}$ )<sup>10</sup>. High in-plane thermal conductivity arises from tight covalent sp<sup>2</sup> bonding between carbon atoms and its unique 2D nature that allows out of plane atomic displacement known as flexural phonons with low energy<sup>11</sup>. Graphene's  $\pi$ -orbitals create a densely delocalized electron cloud that effectively fills the gaps within its aromatic rings (Figure 2). As a result, this generates a repulsive field, preventing the passage of even the smallest molecules, such as hydrogen and helium, endowing graphene with its outstanding impermeability<sup>12</sup>. Finally, the unique electronic band structure of graphene, formed by the delocalized  $\pi$ -orbitals, explains its exceptional electron mobility. This band structure allows electrons to move nearly unimpeded, resulting in high electrical conductivity<sup>13</sup>.

In the past few years, there has been a significant increase in the utilization of graphene in anticorrosive coatings driven by the desire to exploit its exceptional qualities listed previously, notably its impermeability<sup>14-17</sup>. Although extensive efforts have been made to understand the role of graphene in pure graphene and graphene-based composite

coatings using experimental and computational methods such as quantum chemistry and molecular simulation<sup>18</sup>, there still exists controversy surrounding its true potential<sup>19,20</sup>. Furthermore, the availability of a wide range of graphene materials with diverse morphologies and properties, coupled with the potential for numerous chemical modifications, has led to fluctuating performance data reported in the literature using the umbrella term "graphene"<sup>21</sup>. As a matter of fact, the points discussed earlier have the potential to create confusion among end-users in the paint industry who may not be familiar with nanotechnology. This study starts by clarifying the terminology surrounding graphene for the benefit of the end users. The second part reviews various applications of graphene in coatings. Next, focusing on graphene composite coatings, main anticorrosive mechanisms attributed to graphene are elucidated. Both promising results and drawbacks reported in the literature are also discussed. Following this, the main reasons contributing to the unsuccessful attempts of end-users to apply graphene are enumerated and described. Finally, graphene composite coating applications are presented, emphasizing the significant potential offered by graphene-based anticorrosive additives.

## 2. Graphene Terminology Ambiguity

The term 'graphene' is commonly used to refer to a single layer of graphene. However, in the literature, other graphene-based materials are also often included under the same umbrella designation. Based on the number of graphene layers, the following name reported in Table 2 are typically used in the literature.

In general, the term 'few-layer graphene' refers to a material consisting of several graphene layers, typically less than 10 layers. On the other hand, 'Graphene Nanoplatelets' or 'Graphene Nanosheets' allude to nanoparticles composed of more than 10 stacked graphene layers. The term 'Multilayer' graphene can be confusing in this context. The number of graphene layers is a crucial indicator of the material's performance, as its properties tend to decline with an increasing number of graphene layers. For instance, electronic properties of 2D graphene-layered materials do not remain distinct from those of graphite (bulk material) beyond 10 layers<sup>31</sup>.

\*e-mail: [xavier.raby@gerdaugraphene.com](mailto:xavier.raby@gerdaugraphene.com)

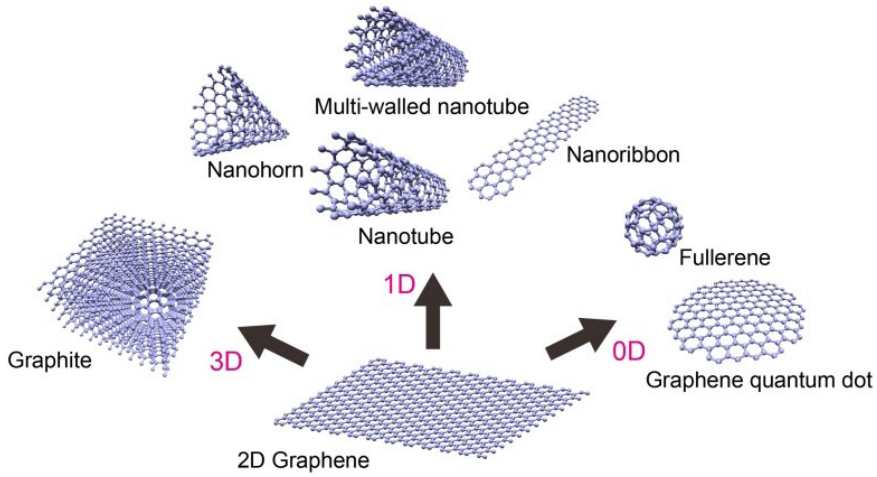


Figure 1.  $sp^2$  hybridized carbon allotropes<sup>7</sup>.

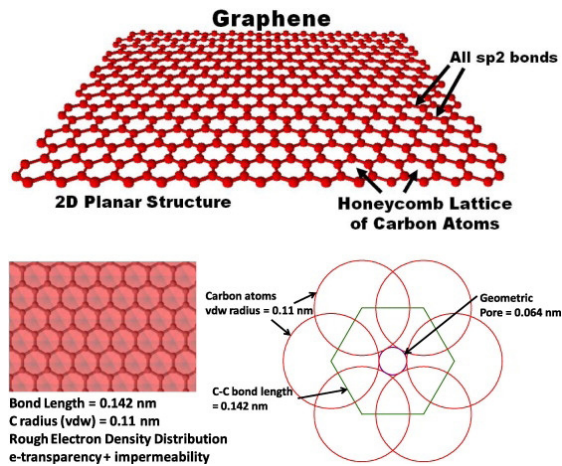


Figure 2. Graphene lattice structure<sup>11</sup>.

Table 1. Graphene amazing physical properties<sup>8</sup>.

Basic properties	Graphene	Other material
Young's modulus	1100 GPa	250 GPa (Steel)
Electrical conductivity	100 MS.m <sup>-1</sup>	60 MS.m <sup>-1</sup> (Copper)
Thermal conductivity	5000 W.m <sup>-1</sup> .K <sup>-1</sup>	2200 W.m <sup>-1</sup> .K <sup>-1</sup> (Diamond)

Table 2. Graphene-like material name according to layer number and thickness.

Name	Layer number	Thickness	Sources
Few-Layer Graphene	2 – 5	-	22,23
Few-Layer Graphene	2 – 10	-	24
Few-Layer Graphene	5 – 10	-	25
Multilayer Graphene	2 – 10	-	22,23,26
Multilayer Graphene	20 – 30	-	25
Multilayer Graphene	>10	-	27
Graphene Nanoplatelets	>10	-	22,27,28
Graphene Nanoplatelets	10 - 30	-	29
Graphene Nanoplatelets	-	0,34 – 100nm	30
Graphene Nanosheets	>10	< 100nm	24

The same behaviour is observed for thermal conductivity, which drops beyond 4 layers to a level that graphite can reach<sup>32</sup>. Nevertheless, this trend is not observed in the same amplitude for all graphene properties, for example, marginal differences in mechanical properties are measured from 3 to 7 layers<sup>33</sup>. In general, one must carefully assess the required performance versus cost-effectiveness (Table 3) for each graphene application. For instance, when considering gas barrier in polymer matrix, the best results are not always achieved with the thinnest graphene, as other morphological properties, such as lateral size and particle size distribution, can play a more significant role<sup>34</sup>.

Another aspect of graphene terminology that can be confusing is the distinction between pristine graphene, graphene oxide and reduced graphene oxide, which is not always very clear (Figure 3). Graphene oxide (GO) stands out as a distinctive material, essentially a single monomolecular layer of graphene, enriched with diverse oxygen-containing functionalities like epoxide, carboxyl, and hydroxyl groups. Upon appropriate reduction, reduced graphene oxide (rGO) emerges, sharing similarities with graphene, yet retaining residual oxygen and heteroatoms, alongside structural imperfections<sup>36</sup>. The presence of those crystalline defects leads to a drop in electrical and thermal properties compared to graphene, GO is considered as insulant while rGO is still considered as electrically conductive<sup>37</sup>. When incorporated as nanofillers in a polymer matrix, GO and rGO usually exhibit better compatibility with polymer host and may even be covalently bonded

to the matrix<sup>38</sup>. They can be used as reinforcing agent in polymer nanocomposites<sup>39</sup> or adhesion promotor between coatings and substrate<sup>40</sup>.

In general, graphene oxide (GO) is produced using one of several methods, including the Brodie method<sup>41</sup>, the Staudenmaier method<sup>42</sup>, the Hummers method<sup>43</sup>, or variations thereof. All three methods entail the oxidation of graphite to different degrees. The Brodie and Staudenmaier methods involve a combination of potassium chlorate (KClO<sub>3</sub>) and nitric acid (HNO<sub>3</sub>) to oxidize graphite. In contrast, the Hummers method utilizes potassium permanganate (KMnO<sub>4</sub>) and sulfuric acid (H<sub>2</sub>SO<sub>4</sub>) for graphite treatment. rGO is obtained from chemically or thermally treated graphene oxide. Among the commonly employed reducing agents for converting graphene oxide (GO) into rGO, hydrazine, hydrazine hydrate, l-ascorbic acid, and sodium borohydride stand out as the primary choices<sup>44</sup>. Sustainability is highly concerned due to the drawbacks associated with conventional thermal and chemical reduction techniques. These methods demand elevated temperatures and involve the use of hazardous agents, leading to significant energy consumption and the emission of environmentally detrimental pollutants<sup>45</sup>.

**Table 3.** Price order of magnitude per graphene layer<sup>34</sup>.

Layer number	Price Index
1 - 2	10 <sup>5</sup>
>8	1

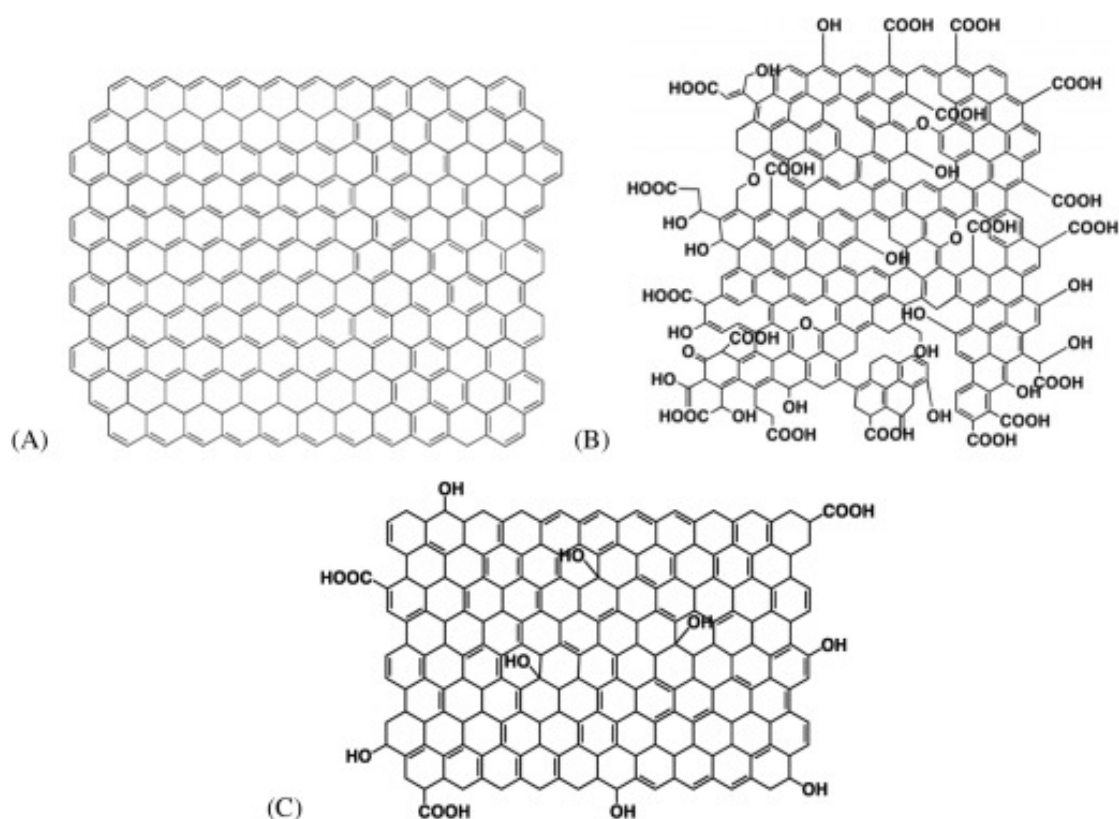


**Figure 3.** Representative structures of (A) graphene, (B) graphene oxide, and (C) reduced graphene oxide<sup>35</sup>.

Furthermore, several technical challenges remain to be addressed in order to facilitate the worldwide industrial availability and economic feasibility of both graphene oxide (GO) and reduced graphene oxide (rGO) when compared to non-oxidised graphene-based materials<sup>46</sup>. The remainder of this study exclusively concentrates on graphene and does not address GO or rGO.

### 3. Graphene in Anticorrosive Coatings Review

#### 3.1. Pure graphene coatings

Thanks to its exceptional impermeability properties mentioned earlier, graphene is a proper candidate for building atom thick coatings onto metals to protect them against corrosion<sup>47</sup>. Moreover, mechanical properties such as microhardness, wear resistance and tribological properties of graphene coated metal can also be enhanced<sup>48</sup>. Among existing methods, chemical vapour deposition (CVD) is the most promising in terms of industrial scalability, quality, graphene coverage and cost effectiveness<sup>49</sup>. Excellent results for protection of metals or alloys made of nickel and copper are reported in the literature with pure graphene coating obtained by CVD method<sup>50</sup>. However, many studies have shown the opposite<sup>51</sup>. While pure graphene coatings can effectively prevent corrosive media from coming into contact with the metallic substrates, the inherent defects in the graphene basal plane caused during the deposition process may disrupt this protection by providing permeation pathways. This can lead to an acceleration of metal corrosion due to micro-galvanic corrosion<sup>52</sup> as illustrated in Figure 4 or the entrapment of chlorine ions in between graphene flakes<sup>54</sup>. In conclusion, even if CVD method is promising, there remains significant industrial challenges to address,

such as defect-free pure graphene coatings production at high scale and at affordable cost<sup>50</sup>.

#### 3.2. Graphene composite coatings

Another approach to using graphene as an anticorrosive enhancer involves dispersing graphene as filler particles within the coating matrix to create graphene composite anticorrosive coatings. Unlike pure graphene coatings, in this case, the preparation and processing of these graphene composite coatings can be aligned with traditional coatings production methods and do not require significant specific adjustments. Numerous studies in the literature have demonstrated positive outcomes supporting the use of graphene in composite coatings. For instance, Sun et al.<sup>55</sup> highlighted an increase by one order of magnitude through electrochemical impedance measurement in an epoxy coating reinforced with just 0.01% wt.% of graphene functionalized with polydimethylsiloxane. The incorporation of graphene sheets in epoxy coatings not only enhances corrosion resistance but also improves surface hydrophobicity and water uptake resistance<sup>56</sup>. In epoxy zinc rich coatings, graphene can function as a zinc sacrificial anode-based protection enhancer, resulting in the reduction of zinc particles while maintaining or improving corrosion performances<sup>57</sup>. However, it is essential to examine these impressive results with caution as some authors revealed certain drawbacks. It is often reported that an excess of graphene in the composite could accelerate corrosion, Wang et al.<sup>58</sup>, reported a reduction in corrosion resistance beyond 1 wt.%. Most authors attribute this phenomenon to the greater tendency for graphene to agglomerate at higher concentrations<sup>59</sup>. Finally, it is also mentioned that graphene sheets alone in composite coating do not improve corrosion resistance in the scribe or cut area when exposed to weathering tests such as salt spray<sup>20</sup>.

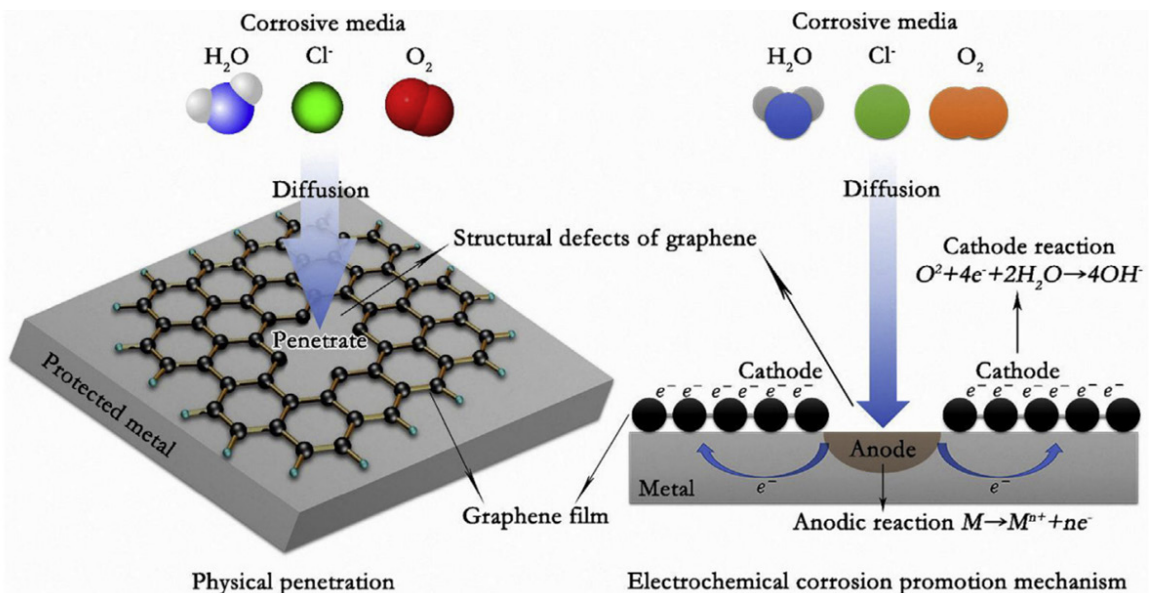


Figure 4. Galvanic corrosion occurring in the defects of pure graphene coating<sup>53</sup>.

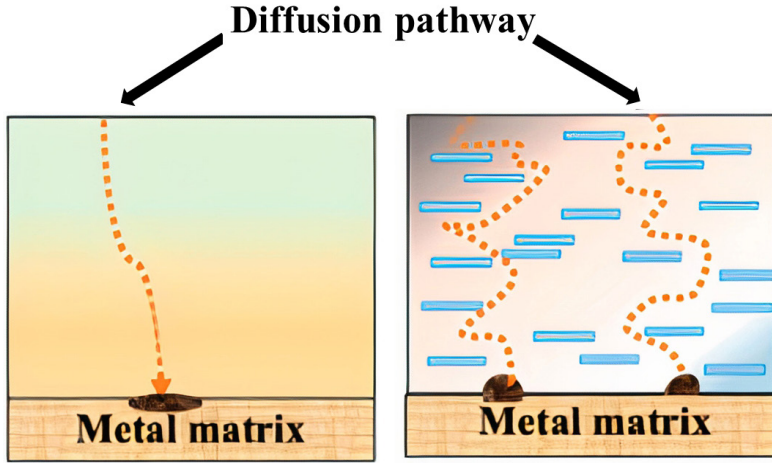


Figure 5. Graphene barrier effect. Adapted from<sup>60</sup>.

## 4. Graphene Composite Coatings in Real-Life Applications

### 4.1. Anticorrosive mechanisms

Superior graphene composite coatings anticorrosion properties can be attributed to two main factors. First, thanks to its high impermeability properties, graphene nanofillers act as a barrier in the coating which slows down the penetration and the diffusion of the corrosion media in the coating. This “barrier effect” makes the path through polymeric matrix much more tortuous for the corrosive species such as water, oxygen, chloride and hydrogen ions to reach the metallic substrate (Figure 5) and consequently reduces the permeability of graphene composite coatings.

In addition to its high impermeability, the high aspect ratio (Equation 1) of the graphene sheets is a also advantageous regarding other lamellar particles<sup>61</sup>.

$$\text{Aspect ratio: } \alpha = \frac{L}{W} \text{ Equation 1}$$

where L is the average lateral size and W thickness of the sheet.

Permeation of penetrants in coatings is governed by both diffusion and solubility mechanisms that takes place in response to pressure gradient across the polymeric film<sup>62</sup>. Based on Nielsen model, permeability (P) can be expressed as the product of solubility and diffusion coefficient which only depends on filler volume fraction ( $\phi$ ) and path tortuosity ( $\tau$ )<sup>63</sup>:

$$\frac{P}{P_0} = \frac{1-\phi}{\tau} \text{ Equation 2}$$

where  $P_0$  is the permeability of the pure polymer matrix.

Path tortuosity in coatings can be expressed as a function of aspect ratio ( $\alpha$ ) and sheet orientation factor ( $S'$ )<sup>64</sup>:

$$\tau = 1 + \frac{2}{3} \alpha \phi \left( S' + \frac{1}{2} \right) \text{ Equation 3}$$

$S'$  represents the orientation of graphene sheets as shown in Figure 6.

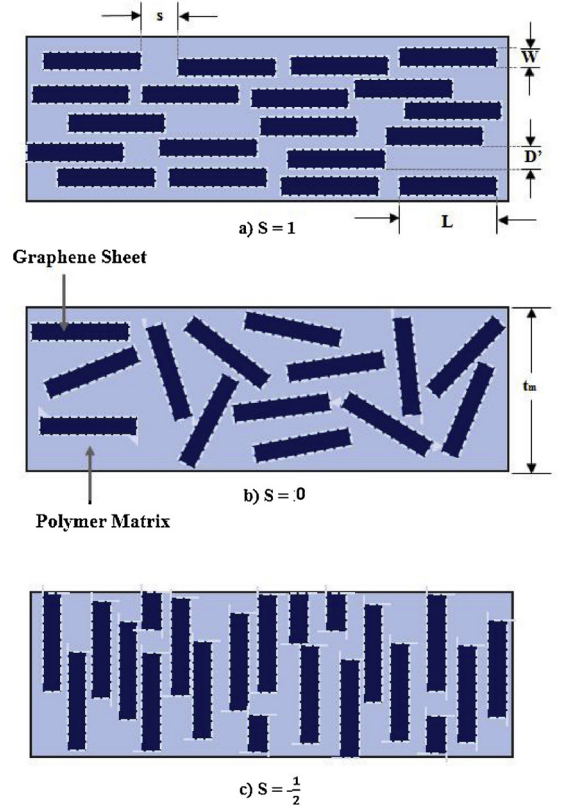


Figure 6. Sheet orientation factor ( $S'$ )<sup>65</sup>.

This mathematic model clearly emphasizes that barrier effect is primarily influenced by graphene volume fraction in the coatings, its aspect ratio and orientation. Beyond these factors, the lateral size distribution is also a key parameter to ensure a high packing density. Indeed, in a randomly arranged system, a graphene with a broad lateral size distribution can better fill up the interspaces between the adjacent flakes<sup>66</sup>. One can see in the Figure 7 that the path tortuosity with broader lateral size distribution is higher than in a uniform one.

Secondly, anticorrosive properties conferred by graphene are directly linked to its electrical conductivity when incorporated in zinc-rich coatings. As the binder in the coating is rarely conductive, a significant proportion of isolated zinc particles cannot act as sacrificial anode because they are not in contact with metal substrate. Graphene behaves as a zinc-rich coatings enhancer through two actions: serving as a cathode of the isolated zinc powder particles and making conductive bridges between metal substrate and zinc particles. Thus, in the first stage, corrosive penetrants can react far before reaching cathodic metal substrate, when it contacts a graphene sheet/zinc particles galvanic couple in the coating. In the second stage, the generated insoluble corrosion product fills the permeation channel improving the barrier properties of the coating but impeded electronic flow between zinc anode and cathodic metallic substrate (Figure 8a). In the case of graphene composite coatings (Figure 8b), even if resulting corrosion product is electrically insulant, a large conductive network between metallic substrate, zinc particles and graphene flakes keeps sacrificial anode reaction occurring during corrosive environment exposure<sup>68</sup>. In addition, the presence of graphene flakes could improve the barrier

effect by making diffusion paths of corrosive species more tortuous to reach the metallic substrate. Thus, barrier effect contributes to reduce the oxidation rate of zinc particles to keep sacrificial anode protection active for a longer period.

#### 4.2. Primary reasons of unsuccessful attempts of end-users to apply graphene

As mentioned earlier, while graphene is often cited in the literature for its anticorrosive properties, it is crucial for graphene end-users to pay special attention to the following points during graphene application in coatings:

- Quality of supplied graphene
- Graphene dosage in coatings
- Graphene dispersion level
- Corrosion in the cut area
- Side effects due to graphene dispersion contaminants

##### 4.2.1. Quality of supplied graphene

Regardless of the source of the graphene, a characterization including the assessment of the crystallinity level, number of graphene layers and lateral size is recommended before utilization. ISO TS 80004<sup>69</sup> and ABNT ISO/TR19733<sup>70</sup>

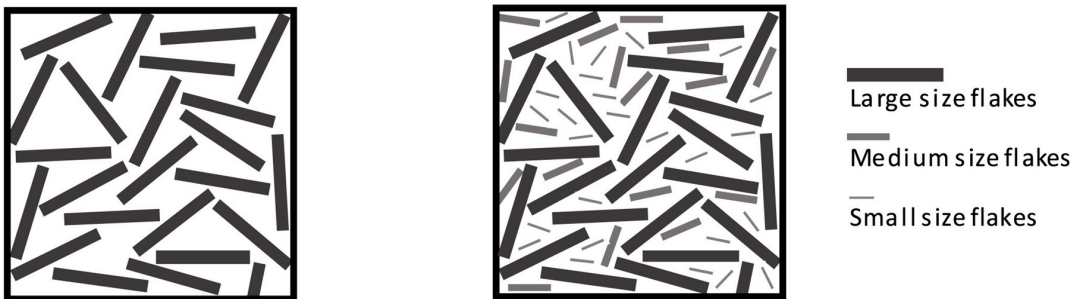


Figure 7. Lateral size distribution impact on path tortuosity<sup>66</sup>.

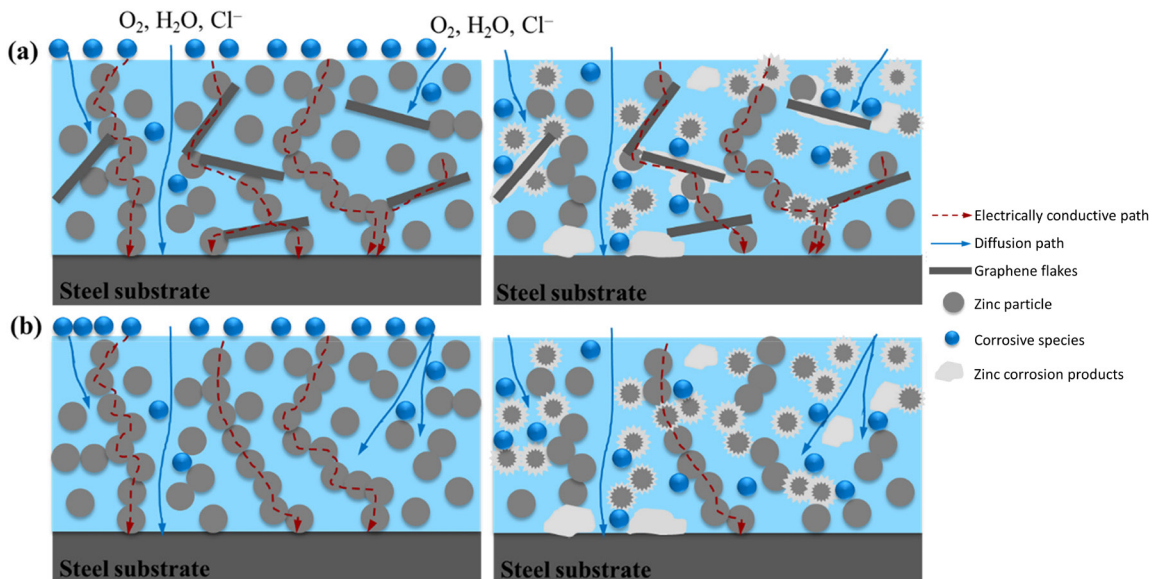


Figure 8. Graphene composite zinc-rich coatings: (a) without graphene, (b) with graphene. Adapted from<sup>67</sup>.

outline and standardize the suitable analytical techniques for characterizing graphene and 2D materials. Poor performances in coatings may arise from the use of a material falsely labelled as graphene.

#### 4.2.2. Graphene dispersion level

Graphene sheets have high surface and excess surface energy, therefore they tend to agglomerate to minimize this energy. Intermolecular interactions between primary graphene platelets easily arise as a consequence of Van der Waals forces. Due to its unique structure of stacked layers of  $sp^2$ -hybridized carbon atoms arranged in a honeycomb pattern, graphene sheets are prone to establish  $\pi$ - $\pi$  stacking interactions<sup>71</sup>. Even though, they are considered as being part of Van der Waals interactions,  $\pi$ - $\pi$  stacking interactions are stronger than typical Van der Waals forces<sup>72</sup> (Table 4). The process of dispersion consists in breaking up agglomerates into primary particles without crushing them into smaller units<sup>73</sup>. In the case of graphene, since  $\pi$ - $\pi$  stacking interactions predominate, de-agglomeration step demands more energy compared to other nanoparticle aggregates that are only governed by typical Van der Waals forces. Dispersion of graphene poses one of the most significant technical challenges in industrial production and should not be underestimated by end-users, as it requires advanced technology beyond the traditional methods for usual coating pigment.

In coatings, the presence of agglomerated graphene sheets can lead to poor anticorrosive properties since the previously described barrier effect is unlikely to occur due to a reduced impermeable area as illustrated in Figure 9.

Moreover, particles agglomerations may result in increasing local PVC/CPVC ratio in the coatings and create local permeation highway for corrosive species<sup>74</sup>.

**Table 4.** Intermolecular interactions relevant to graphene<sup>72</sup>.

Interaction type	Bonding energy (kJ.mol <sup>-1</sup> )
$\pi$ - $\pi$ stacking	8 – 12
Typical Van der Waals	2 – 4

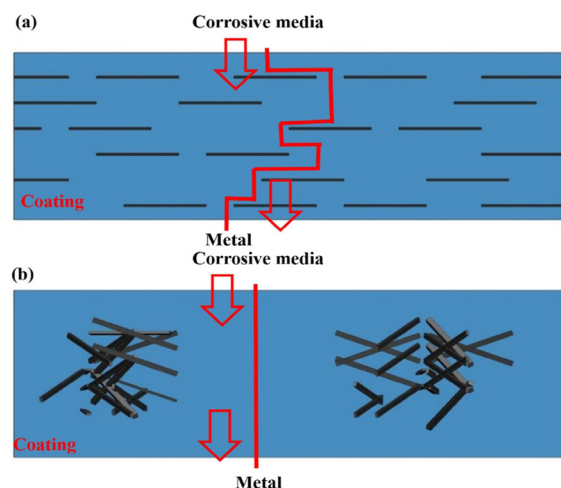


**Figure 9.** Path tortuosity comparison: well dispersed graphene (a) versus poorly dispersed graphene (b)<sup>51</sup>.

#### 4.2.3. Graphene dosage in coatings

Finding the correct graphene dosage is crucial for each coating application. A dosage that is too low may not provide the expected barrier effect, while an excessive amount of graphene could be also detrimental. Indeed, graphene tends to agglomerate at high concentrations<sup>59</sup>. In this case, the same conclusions as described earlier for poorly dispersed graphene (4.2.2) are applicable. In a barrier coating, since graphene is highly conductive, there is a risk of electrical percolation, potentially forming a galvanic couple between metallic substrate and graphene network. Graphene possesses a redox potential higher than most of metallic substrates and can therefore act as a cathode when in contact with them<sup>20</sup>.

#### 4.2.4. Corrosion in the cut area

As mentioned earlier, the main anticorrosive mechanism of graphene is the barrier effect. Therefore, corrosion inhibition in cut area cannot occur when graphene is used alone. In fact, it can even exacerbate the situation if no measure is taken as exemplified in Figure 10. The use of graphene alone cannot replace traditional anodic or cathodic inhibitors.

#### 4.2.5. Graphene dispersion contaminants

It is essential to carefully examine the composition of commercial graphene dispersion due to the presence of contaminants. For example, water soluble compounds can lead to severe blistering in solvent-based coatings after salt spray exposure as displayed in Figure 11.

## 5. Example of Successful Applications

### 5.1. Characterization of solvent based dispersion

Gerdau graphene produces graphene dispersion in several matrices to attend the customer requirements. Xylene matrix is commonly used to ensure a good compatibility with most of solvent-based paints. Gerdau graphene dispersion, denominated as G2D in the rest of the study, has a high solids content (10 wt.%), exhibits a good stability and is characterized hereunder. Substances and methods used for the graphene dispersion process are company proprietary and cannot be detailed here. G2D, after xylene dilution and deposition over a conductive carbon adhesive, were characterized by Scanning Electron Microscopy (SEM) – FEI Quanta 200 FEG. Raman spectroscopy was conducted using a Witec Alpha 300 RA equipment with 532 nm laser. The measured Raman spectra were analyzed using a specific protocol described in<sup>76</sup> to quantify the crystalline defects and the number of graphene coupled interlayers. SEM images (Figure 12) confirm a deagglomerated state of graphene sheets. The overall transparency of the sheets suggests a low thickness. Most of graphene sheets exhibits a lateral size around 2  $\mu$ m. After deposition, Raman map spectroscopy was conducted over 4 areas of 15x15 $\mu$ m in which 8100 graphene spectra were generated. The median spectrum is displayed in Figure 13, the relatively low D band intensity and sharp G band suggest graphene crystallinity is good. The number of Intercoupled graphene layer number is below 10 (Figure 14), this material can be considered as genuine few-layer graphene according to ISO TS 80004.



**Figure 10.** Coating without anodic protection technology after 300 hours salt spray exposure (ASTM B117<sup>75</sup>): increase of corrosion product due to galvanic corrosion between graphene and steel substrate. Left: no graphene. Right: Graphene.



**Figure 11.** Coating after 300 hours salt spray exposure (ASTM B117<sup>75</sup>) Strong osmotic blistering due to water soluble contaminant in graphene dispersion. Right: no graphene. Left: graphene.

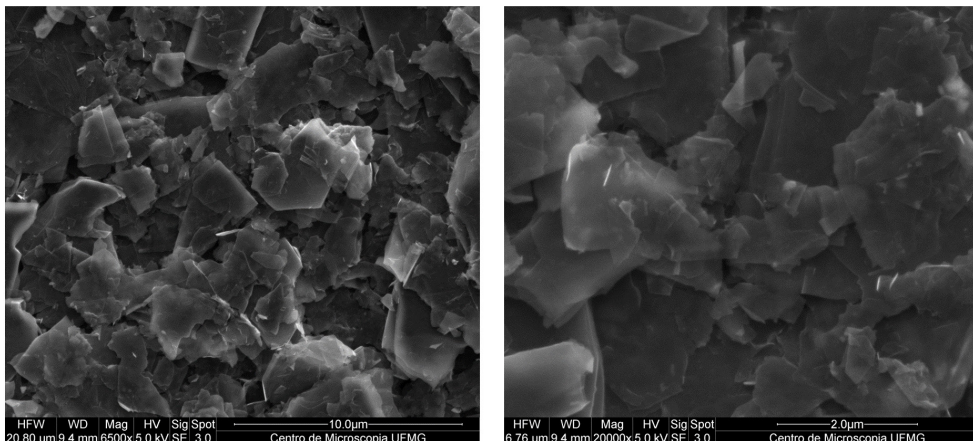


**Figure 12.** SEM images of xylene graphene dispersion.



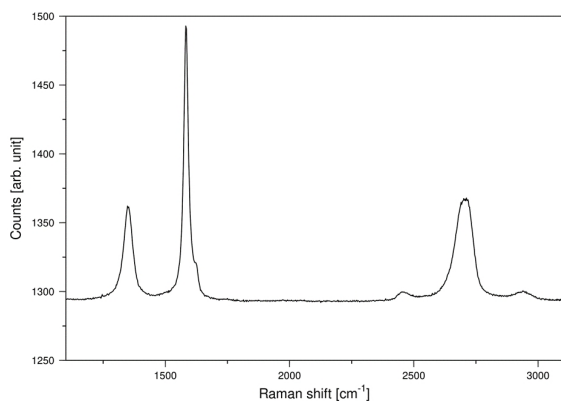


**Figure 13.** Raman median spectrum of xylene graphene dispersion.

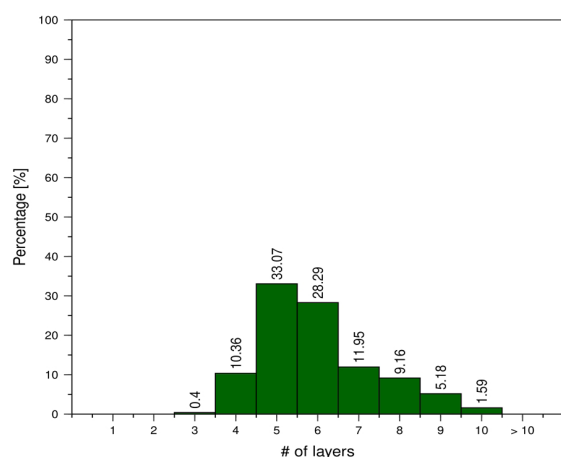


**Figure 14.** Intercoupled layer number distribution.

## 5.2. Application in light maintenance coatings

The previous G2D product was incorporated into the formulation of a solvent-based alkyd/melamine coating to achieve a graphene concentration ranging from 0,05 wt. % and 0,1 wt. % in the liquid paint. Steel metal, coated with a thickness of 50 - 60  $\mu\text{m}$ , were then subjected to salt spray exposure (ASTM B117)<sup>75</sup> for 540h. As demonstrated in Figure 15, the addition of 0,05 to 0,1 wt. % graphene significantly extended the resistance time compared to the reference coating initially designed to withstand 300 hours of exposure. This visual observation highlights the enhanced barrier protection achieved through increased resistance to pore transport as a result of a high dispersion level of graphene flakes within polymeric matrix.

## 5.3. Application in heavy maintenance coatings

### 5.3.1. Barrier epoxy coating

The incorporation of G2D into heavy maintenance barrier epoxy coatings, designed to withstand up to 1500 hours of salt spray exposure (ASTM B117)<sup>75</sup>, prolongs the time needed for the first blistering to show up as depicted in Table 5. This visual inspection is supported by electrochemical impedance spectroscopy (EIS) conducted after 2100 hours of immersion in 3,5 wt.% NaCl at  $22 \pm 2^\circ\text{C}$ , as shown in

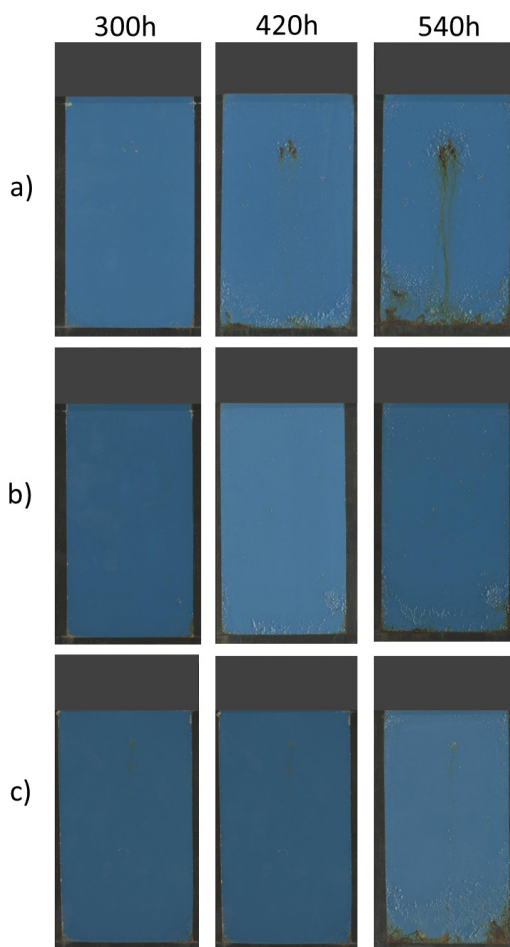


**Figure 15.** Light maintenance coating 300h, 420h and 540h Salt Spray exposure (ASTM B117)<sup>75</sup> (a) Reference without graphene (b) 0.05 wt. % Graphene (c) 0,1 wt. % Graphene.

**Table 5.** Blistering historic.

	Time for the first blistering to show up (h)
Reference	1600
Graphene (0.05 wt. %)	2100

Figure 16. In both cases, although EIS data indicates coatings with high barrier performance, evidenced by elevated values of  $|Z|$  ( $>10^{10}$  ohm.cm<sup>2</sup>) at low frequency and phase angle values close to  $90^\circ$  at high frequency (capacitive behaviour). The difference observed in  $|Z|$  values at low frequency ( $f=0.01\text{Hz}$ ) among the samples (approximately one order of magnitude) suggests an enhanced shielding effect in the graphene-containing sample.

### 5.3.2. Zinc-rich epoxy coatings

G2D was introduced into a zinc-rich epoxy coating in which zinc content was reduced by 25% compared to nominal formulation. Four different graphene concentration were compared: 0; 0,05; 0,1 and 0,25 wt.%. After 2000 hours Salt spray exposure (ASTM B117)<sup>75</sup>, a significant reduction in corrosion was observed in the cut region when the graphene

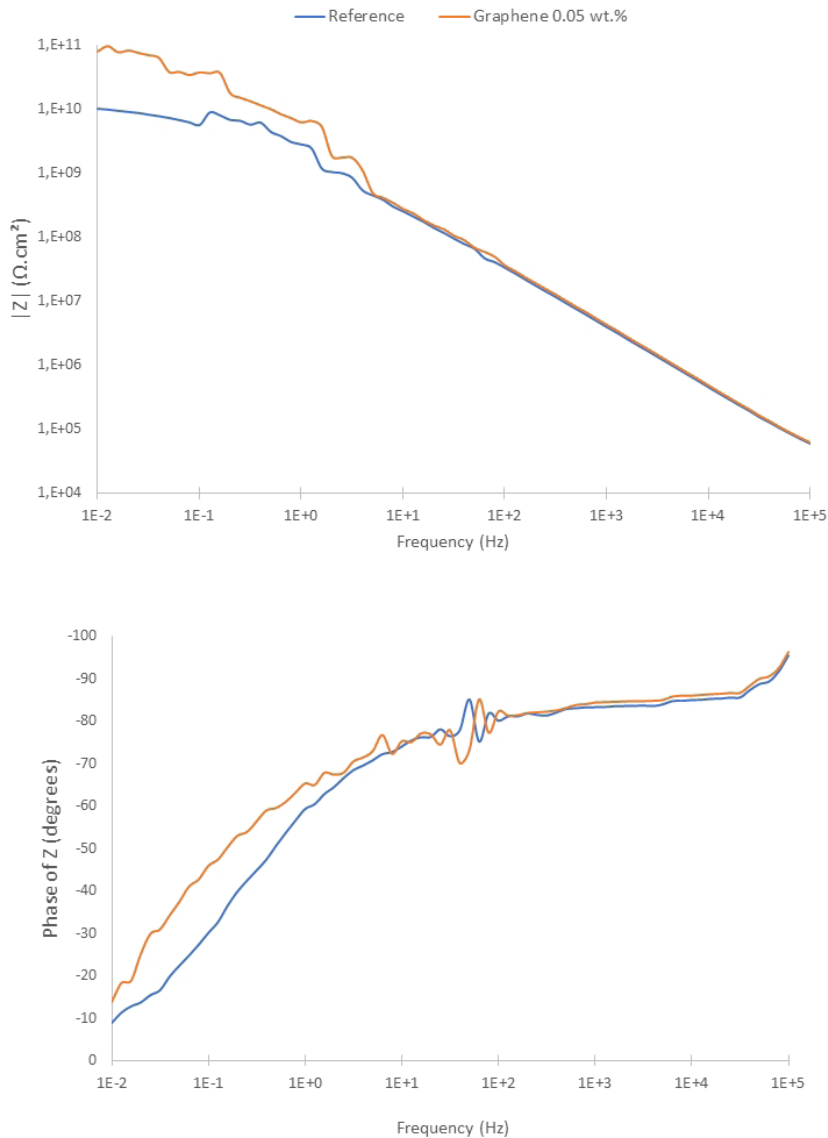


**Figure 16.** EIS after 2100h immersion in 3,5 wt. % NaCl (up: Impedance | bottom: Phase angle).

concentration was increased to 0,25 wt. % as displayed in Figure 17. Despite the reduction in zinc content versus nominal formulation, the decrease in steel corrosion products indicates that the sacrificial anode mechanism was maintained for a longer period of time thanks to the addition of graphene. Indeed, as long as there is sufficient zinc to act as an anode, the steel will be galvanically protected.

## 6. Conclusion and Future Perspectives

A literature review and real-life Graphene-based application examples demonstrate the significant potential of graphene as a new additive enhancer for anticorrosive coating. As a strong barrier, graphene holds significant interest in extending coating shelf life or reducing coating thickness while maintaining performance. Its planar and nanometric morphology with high aspect ratio offers an equivalent shielding effect compared to traditional barrier pigment such as micaceous iron oxide,

glass flakes, mica and others lamellar minerals but at a much lower concentration. Acting as conductive particles with high specific area, graphene emerges as an excellent candidate for significantly reducing the use of metallic zinc in cathodic protection coatings. This leads to optimizations never previously considered including improvements in mechanical properties, adhesion to the substrate, cohesion of the final film, and reduction in paint density for instance. Nevertheless, unlocking the full potential of this material demands specific and favourable conditions that must be carefully followed by the end-user, as misuse can result in adverse outcome. The upcoming years are expected to bring a new generation of graphene-based anticorrosive additives with enhanced performances, combining both strategies:

### a) Graphene chemical covalent functionalization:

Pristine graphene, as presented in this study, interacts only through physical means with the polymeric vehicle into which it is incorporated. Enhancing chemical interactions

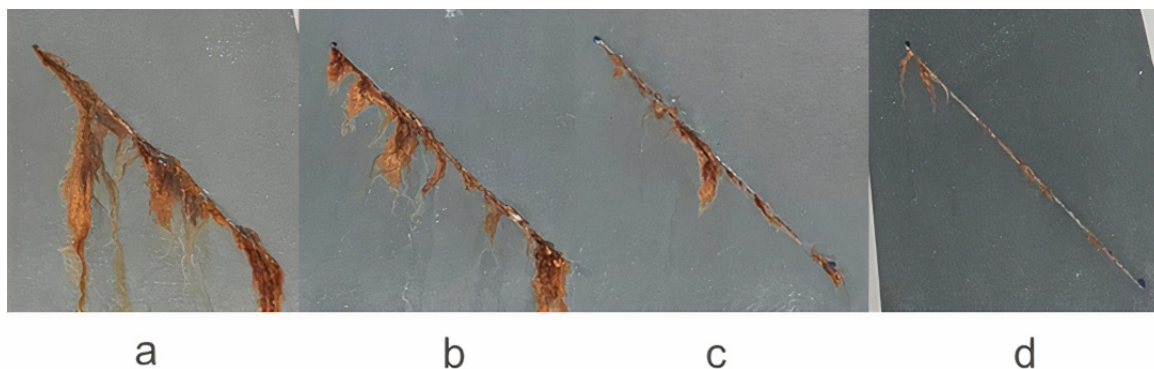


**Figure 17.** Zinc-rich epoxy coatings with reduced zinc content (cut region): graphene concentration in total paint formulation: a) 0 wt. %, b) 0,05 wt. %, c) 0,1 wt. %, d) 0,25 wt.%.

between the nanofiller and the organic matrix through graphene covalent functionalization will lead to better dispersion of graphene and mechanical reinforcement, which is beneficial for improving adhesion properties critical for corrosion resistance.

#### b) Sheet orientation:

The characteristics of the paint or application methods could be optimized to ensure that graphene sheets align more parallel to the substrate, thereby enhancing the efficiency of barrier effect.

## 7. References

- Duplock EJ, Scheffler M, Lindan PJD. Hallmark of perfect graphene. *Phys Rev Lett.* 2004;92(22):225502. <http://dx.doi.org/10.1103/PhysRevLett.92.225502>. PMID:15245234.
- Novoselov KS, Geim AK, Morozov SV, Jiang D, Zhang Y, Dubonos SV, et al. Electric field effect in atomically thin carbon films. *Science.* 2004;306(5696):666-9. <http://dx.doi.org/10.1126/science.1102896>. PMID:15499015.
- Zhang S, Wang H, Liu J, Bao C. Measuring the specific surface area of monolayer graphene oxide in water. *Mater Lett.* 2020;261:127098. <http://dx.doi.org/10.1016/j.matlet.2019.127098>.
- Andreoni W. *The physics of fullerene-based and fullerene-related materials.* Berlin: Springer; 2000.
- Charlier J-C, Blasé X, Roche S. Electronic and transport properties of nanotubes. *Rev Mod Phys.* 2007;79(2):677-732. <http://dx.doi.org/10.1103/RevModPhys.79.677>.
- Novoselov KS, Geim AK, Morozov SV, Jiang D, Zhang Y, Dubonos SV, et al. Electric field effect in atomically thin carbon films. *Science.* 2004;306(5696):666-9. <http://dx.doi.org/10.1126/science.1102896>. PMID:15499015.
- Nakano H, Tetsuka H, Spencer MJS, Morishita T. Chemical modification of group IV graphene analogs. *Sci Technol Adv Mater.* 2018;19(1):76-100. <http://dx.doi.org/10.1080/14686996.2017.1422224>. PMID:29410713.
- Sur UK. Graphene: a rising star on the horizon of materials science. *Int J Electrochem.* 2012;2012:12. <http://dx.doi.org/10.1155/2012/237689>.
- Papageorgiou DG, Kinloch IA, Young RJ. Mechanical properties of graphene and graphene-based nanocomposites. *Prog Mater Sci.* 2017;90:75-127. <http://dx.doi.org/10.1016/j.pmatsci.2017.07.004>.
- Rizzi L, Wijaya AF, Palanisamy LV, Schuster J, Köhne M, Schulz SE. Quantifying the influence of graphene film nanostructure on the macroscopic electrical conductivity. *Nano Ex.* 1:020035. <http://dx.doi.org/10.1088/2632-959X/abb37a>.
- Pop E, Varshney V, Roy AK. Thermal properties of graphene: fundamentals and applications. *MRS Bull.* 2012;37:1273. <http://dx.doi.org/10.1557/mrs.2012.203>.
- Berry V. Impermeability of graphene and its applications. *Carbon.* 2013;62:1-10. <http://dx.doi.org/10.1016/j.carbon.2013.05.052>.
- Castro AH No, Guinea F, Peres NMR, Novoselov KS, Geim AK. The electronic properties of graphene. *Rev Mod Phys.* 2009;81(1):109-62. <http://dx.doi.org/10.1103/RevModPhys.81.109>.
- Chang C-H, Huang T-C, Peng C-W, Yeh T-C, Lu H-I, Hung W-I, et al. Novel anticorrosion coatings prepared from polyaniline/graphene composites. *Carbon.* 2012;50(14):5044-51. <http://dx.doi.org/10.1016/j.carbon.2012.06.043>.
- Li Y, Yang Z, Qiu H, Dai Y, Zheng Q, Li J, et al. Self-aligned graphene as anticorrosive barrier in waterborne polyurethane composite coatings. *J Mater Chem A.* 2014;2:14139-145. <https://doi.org/10.1039/C4TA02262A>.
- Yu Z, Di H, Ma Y, Lv L, Pan Y, Zhang C, et al. Fabrication of graphene oxide–alumina hybrids to reinforce the anticorrosion performance of composite epoxy coatings. *Appl Surf Sci.* 2015;351:986-96. <http://dx.doi.org/10.1016/j.apsusc.2015.06.026>.
- Zhu G, Cui X, Zhang Y, Dong M, Liu H, Shao Q, et al. Poly(vinyl butyral)/graphene oxide/poly methylhydrosiloxane) nanocomposite coating for improved aluminum alloy anticorrosion. *Polymer (Guildf).* 2019;172.
- Zhang R, Yu X, Yang Q, Cui G, Li Z. The role of graphene in anti-corrosion coatings: a review. *Constr Build Mater.* 2021;294:123613. <http://dx.doi.org/10.1016/j.conbuildmat.2021.123613>.
- Lee J, Berman D. Inhibitor or promoter: insights on the corrosion evolution in a graphene protected surface. *Carbon.* 2017;126:225-31. <http://dx.doi.org/10.1016/j.carbon.2017.10.022>.
- Davidson RD, Cubides Y, Fincher C, Stein P, McLain C, Xu B-X, et al. Tortuosity but not percolation: design of exfoliated graphite nanocomposite coatings for extended corrosion protection of aluminum alloys. *ACS Appl Nano Mater.* 2019;2(5):3100-16. <http://dx.doi.org/10.1021/acsnanm.9b00451>.
- Kulyk B, Freitas MA, Santos NF, Mohseni F, Carvalho AF, Yasakau K, et al. A critical review on the production and application of graphene and graphene-based materials in anti-corrosion coatings. *Crit Rev Solid State Mater Sci.* 2021;47(3):309-55. <http://dx.doi.org/10.1080/10408436.2021.1886046>.
- Bianco A, Cheng H-M, Enoki T, Gogotsi Y, Hurt RH, Koratkar N, et al. All in the graphene family – A recommended nomenclature for two-dimensional carbon materials. *Carbon.* 2013;65:1-6. <http://dx.doi.org/10.1016/j.carbon.2013.08.038>.
- Kumar V, Kumar A, Lee D-J, Park S-S. Estimation of number of graphene layers using different methods: a focused review. *Materials (Basel).* 2021;14(16):4590. <http://dx.doi.org/10.3390/ma14164590>. PMID:34443113.

24. Wick P, Louw-Gaume AE, Kucki M, Krug HF, Kostarelos K, Fadeel B, et al. Classification framework for graphene-based materials. *Angew Chem Int Ed*. 2014;53(30):7714-8. <http://dx.doi.org/10.1002/anie.201403335>.
25. Pershin VF, Krasnyanskiy MN, Alhilo ZAA, Al-Mashhadani AMR, Baranov AA, Osipov AA. Production of few-layer and multilayer graphene by shearing exfoliation of graphite in liquids. *IOP Conf Ser Mater Sci Eng*. 2019;693:012023. <http://dx.doi.org/10.1088/1757-899X/693/1/012023>.
26. Salesa B, Tuñón-Molina A, Cano-Vicent A, Assis M, Andrés J, Serrano-Aroca A. Graphene nanoplatelets: in vivo and in vitro toxicity, cell proliferative activity, and cell gene expression. *Appl Sci (Basel)*. 2022;12(2):720. <http://dx.doi.org/10.3390/app12020720>.
27. Kumar D, Singh K, Verma V, Bhatti HS. Microwave assisted synthesis and characterization of graphene nanoplatelets. *Appl Nanosci*. 2016;6(1):97-103. <http://dx.doi.org/10.1007/s13204-015-0415-9>.
28. Wang J, Zhao C, Mark LH, Wang X, Li R, Moghimi N, et al. Facilitating supercritical CO<sub>2</sub> assisted exfoliation of graphene nanoplatelets with the polymer matrix. *Chem Eng J*. 2020;394:124930. <http://dx.doi.org/10.1016/j.cej.2020.124930>.
29. Nieto A, Lahiri D, Agarwal A. Synthesis and properties of bulk graphene nanoplatelets consolidated by spark plasma sintering. *Carbon*. 2012;50(11):2048. <http://dx.doi.org/10.1016/j.carbon.2012.04.054>.
30. Cataldi P, Athanassiou A, Bayer IS. Graphene nanoplatelets-based advanced materials and recent progress in sustainable applications. *Appl Sci (Basel)*. 2018;8(9):1438. <http://dx.doi.org/10.3390/app8091438>.
31. Partoens B, Peeters FM. From graphene to graphite: electronic structure around the K point. *Phys Rev B Condens Matter Mater Phys*. 2006;74(7):075404. <http://dx.doi.org/10.1103/PhysRevB.74.075404>.
32. Yan Z, Nika DL, Balandin AA. Review of thermal properties of graphene and few-layer graphene: applications in electronics. *IET Circuits, Devices and Systems*. 2015;9:4.
33. Zhang YY, Gu YT. Mechanical properties of graphene: effects of layer number, temperature and isotope. *Comput Mater Sci*. 2013;71:197-200. <http://dx.doi.org/10.1016/j.commatsci.2013.01.032>.
34. Zahid M, Esau Del Río Castillo A, Thorat SB, Panda JK, Bonaccorso F, Athanassiou A. Graphene morphology effect on the gas barrier, mechanical and thermal properties of thermoplastic polyurethane. *Compos Sci Technol*. 2020;200:108461. <http://dx.doi.org/10.1016/j.compscitech.2020.108461>.
35. Kumar CV, Pattammattel A. Introduction to graphene: chemical and biochemical applications. Amsterdam: Elsevier; 2017. Chapter 1, Discovery of graphene and beyond; p. 1-15. <http://dx.doi.org/10.1016/B978-0-12-813182-4.00001-5>.
36. Zhu Y, Murali S, Cai W, Li X, Suk JW, Potts JR, et al. Graphene and graphene oxide: synthesis, properties, and applications. *Adv Mater*. 2010;22(35):3906-24. <http://dx.doi.org/10.1002/adma.201001068>. PMID:20706983.
37. Gill FS, Uniyal D, Prasad B, Saluja S, Mishra A, Bachheti RK, et al. Investigation of increased electrical conductivity by rGO in rGO/PVDF/PMMA/PTFE nanocomposites. *J Mol Struct*. 2022;1267:133541. <http://dx.doi.org/10.1016/j.molstruc.2022.133541>.
38. Smith AT, LaChance AM, Zeng S, Liu B, Sun L. Synthesis, properties, and applications of graphene oxide/reduced graphene oxide and their nanocomposites. *Nano Mater Sci*. 2019;1(1):31-47.
39. Papageorgiou DG, Kinloch IA, Young RJ. Graphene/elastomer nanocomposites. *Carbon*. 2015;95:460-84. <http://dx.doi.org/10.1016/j.carbon.2015.08.055>.
40. Li J, Cui J, Yang Y, Ma H, Qiu H, Yang J. Silanized graphene oxide reinforced organofunctional silane composite coatings for corrosion protection. *Prog Org Coat*. 2016;99:443-51. <http://dx.doi.org/10.1016/j.porgcoat.2016.07.008>.
41. Brodie BC. Sur le poids atomique du graphite. *Ann Chim Phys*. 1860;59:466.
42. Staudenmaier L. Verfahren zur Darstellung der Graphitsäure. *Ber Dtsch Chem Ges*. 1898;31(2):1481-7. <http://dx.doi.org/10.1002/cber.18980310237>.
43. Hummers WS Jr, Offeman RE. Preparation of graphitic oxide. *J Am Chem Soc*. 1958;80(6):1339. <http://dx.doi.org/10.1021/ja01539a017>.
44. Lee SS, Paliouras M, Trifiro MA. Functionalized carbon nanoparticles as theranostic agents and their future clinical utility in oncology. *Bioengineering (Basel)*. 2023;10(1):108. <http://dx.doi.org/10.3390/bioengineering10010108>. PMID:36671680.
45. Lee AY, Hwangbo SA, Jeong MS, Lee TG. Eco-friendly sonochemical reduction of graphene oxide in water using TiO<sub>2</sub> photocatalyst activated by sonoluminescence. *Appl Surf Sci*. 2022;605:154820. <http://dx.doi.org/10.1016/j.apsusc.2022.154820>.
46. Lowe S, Zhong YL. Challenges of industrial-scale graphene oxide production: fundamentals and applications. In: Dimiev AM, Eglar S. *Graphene oxide: fundamentals and application*. Hoboken: Wiley; 2016. p. 410-31. <http://dx.doi.org/10.1002/9781119069447.ch13>.
47. Chen S, Brown L, Levendorf M, Cai W, Ju S-Y, Edgeworth J, et al. Oxidation resistance of graphene-coated Cu and Cu/Ni alloy. *ACS Nano*. 2011;5(2):1321-7. <http://dx.doi.org/10.1021/nn103028d>. PMID:21275384.
48. Algul H, Tokur M, Ozcan S, Uysal M, Cetinkaya T, Akbulut H, et al. The effect of graphene content and sliding speed on the wear mechanism of nickel-graphene nanocomposites. *Appl Surf Sci*. 2015;359:340-8. <http://dx.doi.org/10.1016/j.apsusc.2015.10.139>.
49. Vlassiok I, Fulvio P, Meyer H, Lavrik N, Dai S, Datskos P, et al. Large scale atmospheric pressure chemical vapor deposition of graphene. *Carbon*. 2013;54:58-67. <http://dx.doi.org/10.1016/j.carbon.2012.11.003>.
50. Kakaei K, Esrafil MD, Ehsani A. Graphene and anticorrosive properties. *Interface Sci Technol*. 2019;27:303-37. <http://dx.doi.org/10.1016/B978-0-12-814523-4.00008-3>.
51. Cui G, Bi Z, Zhang R, Liu J, Yu X, Li Z. A comprehensive review on graphene-based anti-corrosive coatings. *Chem Eng J*. 2019;373:104-21. <http://dx.doi.org/10.1016/j.cej.2019.05.034>.
52. Hsieh YP, Hofmann M, Chang KW, Jhu JG, Li YY, Chen KY, et al. Complete corrosion inhibition through graphene defect passivation. *ACS Nano*. 2014;8(1):443-8. <http://dx.doi.org/10.1021/nn404756q>. PMID:24359599.
53. Ding R, Li W, Wang X, Gui T, Li B, Han P, et al. A brief review of corrosion protective films and coatings based on graphene and graphene oxide. *J Alloys Compd*. 2018;764:1039-55. <http://dx.doi.org/10.1016/j.jallcom.2018.06.133>.
54. Lee J, Berman D. Inhibitor or promoter: insights on the corrosion evolution in a graphene protected surface. *Carbon*. 2018;126:225-31. <http://dx.doi.org/10.1016/j.carbon.2017.10.022>.
55. Sun W, Wang L, Yang Z, Zhu T, Wu T, Dong C, et al. A facile method for the modification of graphene nanosheets as promising anticorrosion pigments. *Mater Lett*. 2018;228:152-6. <http://dx.doi.org/10.1016/j.matlet.2018.05.105>.
56. Abakah RR, Huang F, Hu Q, Wang Y, Liu J. Comparative study of corrosion properties of different graphene nanoplate/epoxy composite coatings for enhanced surface barrier protection. *Coatings*. 2021;11(3):285. <http://dx.doi.org/10.3390/coatings11030285>.
57. Cao X, Huang F, Huang C, Liu J, Cheng YF. Preparation of graphene nanoplate added zinc-rich epoxy coatings for enhanced sacrificial anode-based corrosion protection. *Corros Sci*. 2019;159:108120. <http://dx.doi.org/10.1016/j.corsci.2019.108120>.
58. Wang X, Qi X, Lin Z, Battocchi D. Graphene reinforced composites as protective coatings for oil and gas pipelines.

- Nanomaterials (Basel). 2018;12(12):1005. <http://dx.doi.org/10.3390/nano8121005>. PMID:30518068.
59. Kopsidas S, Olowojoba GB, Kinloch AJ, Taylor AC. Examining the effect of graphene nanoplatelets on the corrosion resistance of epoxy coatings. *Int J Adhes Adhes*. 2021;104:102723. <http://dx.doi.org/10.1016/j.ijadhadh.2020.102723>.
  60. Abakah RR, Huang F, Hu Q, Wang Y, Liu J. Comparative study of corrosion properties of different graphene nanoplate/epoxy composite coatings for enhanced surface barrier protection. *Coatings*. 2021;3(3):285. <http://dx.doi.org/10.3390/coatings11030285>.
  61. Kausar A. Applications of polymer/graphene nanocomposite membranes: a review. *Mater Res Innov*. 2018;26:1.
  62. Cui Y, Kundalwal SI, Kumar S. Gas barrier performance of graphene/polymer nanocomposites. *Carbon*. 2016;98:313-33. <http://dx.doi.org/10.1016/j.carbon.2015.11.018>.
  63. Nielsen LE. Models for the permeability of filled polymer systems. *J Macromol Sci: Pt A - Chem*. 1967;1(5):929-42.
  64. Manias E. Polymer nanocomposite technology, fundamentals of barrier. In: TAPPI-2009: Flexible Packaging, Nanotechnology Symposium Book; 2009; USA. Peachtree Corners: TAPPI; 2009. p. 1-6. (art.no.1/keynote).
  65. Othman NH, Ismail MC, Mustapha M, Sallih N, Kee KE, Jaal RA. Graphene-based polymer nanocomposites as barrier coatings for corrosion protection. *Prog Org Coat*. 2019;135:82-99. <http://dx.doi.org/10.1016/j.porgcoat.2019.05.030>.
  66. Zahid M, Castillo AEDR, Thorat SB, Panda JK, Bonaccorso F, Athanassiou A. Graphene morphology effect on the gas barrier, mechanical and thermal properties of thermoplastic polyurethane. *Compos Sci Technol*. 2020;200:108461. <http://dx.doi.org/10.1016/j.compscitech.2020.108461>.
  67. Qi C, Dam-Johansen K, Weinell CE, Bi H, Wu H. Enhanced anticorrosion performance of zinc rich epoxy coatings modified with stainless steel flakes. *Prog Org Coat*. 2022;163:106616. <http://dx.doi.org/10.1016/j.porgcoat.2021.106616>.
  68. Ding R, Zheng Y, Yu H, Li W, Wang X, Gui T. Study of water permeation dynamics and anti-corrosion mechanism of graphene/zinc coatings. *J Alloys Compd*. 2018;748:481-95. <http://dx.doi.org/10.1016/j.jallcom.2018.03.160>.
  69. ISO: International Organization for Standardization. [Internet]. ISO 80004-1:2023 Nanotechnologies. Geneva: ISO; 2023 [cited 2023 November 30]. Available from: [www.iso.org](http://www.iso.org)
  70. ABNT: Associação Brasileira de Normas Técnicas. [Internet]. ABNT ISO/TR 19733-1:2023 Nanotecnologias — Matriz de propriedades e técnicas de medição para grafeno e materiais bidimensionais (2D) relacionados. Rio de Janeiro: ABNT; 2023 [cited 2023 November 30]. Available from: [www.abnt.org.br](http://www.abnt.org.br)
  71. Perez E, Martín N.  $\pi$ - $\pi$  interactions in carbon nanostructures. *Chem Soc Rev*. 2015;44(18):6425-33. <http://dx.doi.org/10.1039/C5CS00578G>. PMID:26272196.
  72. Hu K, Kulkarni DD, Choi I, Tsukruk VV. Graphene-polymer nanocomposites for structural and functional applications. *Prog Polym Sci*. 2014;39(11):1934-72. <http://dx.doi.org/10.1016/j.progpolymsci.2014.03.001>.
  73. Wicks ZJ, Jones N, Pappas P. Pigment dispersion: 1. *J Coatings Technology*. 2001;145-49.
  74. Bierwagen G. The physical chemistry of organic coatings revisited: viewing coatings as a materials scientist. *J Coat Technol Res*. 2008;5(2):133-55. <http://dx.doi.org/10.1007/s11998-007-9066-4>.
  75. ASTM: American Society for Testing and Materials. ASTM B117-19: standard practice for operating salt spray (Fog) apparatus. West Conshohocken: ASTM; 2019. <http://dx.doi.org/10.1520/B0117-19>.
  76. Silva DL, Campos JLE, Fernandes TFD, Rocha JN, Machado LRP, Soares EM, et al. Raman spectroscopy analysis of number of layers in mass-produced graphene flakes. *Carbon*. 2020;161:181-9. <http://dx.doi.org/10.1016/j.carbon.2020.01.050>.